Limnol. Oceanogr., 51(2), 2006, 847–859

Physical and biogeochemical controls of microaggregate dynamics in a tidally affected coastal ecosystem

Mirko Lunau,[1] *Andreas Lemke, Olaf Dellwig, and Meinhard Simon*
Institute for Chemistry and Biology of the Marine Environment, University of Oldenburg, P.O. Box 2503, D-26111 Oldenburg, Germany

Abstract

Tidal flat ecosystems exhibit pronounced tidal currents that cause high loads of suspended matter (SPM) and intense sedimentation. To identify systematic patterns of tidal SPM dynamics and the significance of physical forcing versus microbial processes in aggregation processes, we conducted a comprehensive study from January 2002 to October 2004 in a backbarrier tidal flat area of the German Wadden Sea. Further, various aggregate fractions were separated by their settling properties in June and October 2004, applying a new sampling device. Tidal dynamics of SPM, particulate organic carbon (POC), aggregate abundance and size, chlorophyll *a* (Chl *a*), the carbon to nitrogen ratio (C : N), numbers of bacteria, and DOC often exceeded seasonal dynamics of the tidal means of these properties. SPM, POC, Chl *a*, and aggregate abundance were positively correlated and aggregate size negatively correlated to the current. DOC concentrations and total bacterial numbers exhibited minima at high tide and maxima at low tide. Aggregate quality—i.e., POC : SPM, Chl *a*, size, amino acid content, and bacterial colonization—varied tidally among the fractions, relative to bulk SPM and was different in June and October. In June, tidal dynamics of these properties and bacterial biomass production were higher than in October. Aggregate abundance was substantially lower during the growing season and aggregate size larger than in fall and winter. Microbial processes were important during the growing season in affecting tidal dynamics of aggregation and sedimentation, whereas in fall and winter, physical forcing was the main factor controlling aggregate dynamics.

Tidal flat ecosystems at the transition zone between land and coastal seas are strongly affected by inputs of inorganic nutrients and organic matter both from terrestrial as well as marine origin and thus are one of the most productive marine ecosystems. They act as a filter and sink for a variety of land-born substances running off the coast and are, together with estuaries, of prime importance in land–sea interactions. They exhibit pronounced tidal currents whose dynamics cause intense sedimentation and resuspension of particulates, resulting in permanently turbid water masses with high loads of suspended matter (SPM). Phytoplankton primary production is strongly light-limited and rather low and benthic primary production contributes substantial amounts (Tillmann et al. 2000; Wolfstein et al. 2000). Because of the high input of organic matter, tidal flat ecosystems are usually net-heterotrophic and act as a sink for organic matter (Postma 1981). Despite this high input of organic matter, the SPM is dominated largely by inorganic constituents, and most of it is composed of microaggregates <500 μm, undergoing pronounced changes and restructuring during current velocity changes (Eisma and Li 1993; Chen et al. 1994; Mikkelsen and Pejrup 1998). At slack water, rather low SPM concentrations occur because substantial amounts of the SPM settle out. Differential settling appears to be the most important mechanism to generate rather large aggregates at this time of low shear rates. At mean tide and towards the current velocity maximum (CVM), when high shear rates occur, resuspension results in high concentration of SPM, composed of rather small aggregates (<100 μm).

Besides these dramatic changes of aggregate dynamics during tidal cycles, seasonal variations in SPM concentration and composition and in the aggregate size structure have been reported (Behrends and Liebezeit 1999; Mikkelsen 2002; Grossart et al. 2004). It is, however, not well understood how physical forcing—i.e., the flow field—and biological properties of the component particles, aggregates, and the dissolved phase interact and control aggregate dynamics seasonally, but also during tidal cycles. We do not know whether the various fractions of aggregates, differing in size, sticking and settling properties, vary in their biochemical and geochemical composition. Diatoms and bacteria produce mucus material, which affect aggregation (Passow 2002; Bhaskar et al. 2005). Further, diatom species vary in their stickiness and aggregation properties (Kiørboe and Hansen 1993; Passow and Alldredge 1995), and adsorption properties of dissolved organic carbon (DOC)—i.e., the hydrophobicity—in tidal flat systems undergo pronounced seasonal changes (Bakker et al. 2003). We hypothesize that these and other properties are important—but so far neglected—in controlling and thus understanding dynamics of aggregate formation and sedimentation in tidal flat ecosystems.

The role of heterotrophic bacteria in the turnover of organic matter on aggregates has been studied quite extensively during the last decade (*for review see* Simon et al. 2002). Most of these studies have been carried out in pelagic systems, but rivers and estuaries have been studied as well.

[1] Corresponding author: (lunau@icbm.de).

Acknowledgments

We thank O. Axe, C. Duerselen, J. Freund, L. Gansel, H. P. Grossart, O. Joerdel, C. Klotz, S. Kotzur, B. Kuerzel, J. Maerz, B. Rink, F. Roelfs, A. Schlingloff, A. Sommer, E. Stanev, R. Weinert, M. Zarubin, and the captain and crew of RV *Senckenberg* for technical assistance in the field and in the lab and for excellent cooperation. We also thank the marine physics group, University of Oldenburg, for providing the data from the measuring pole. This work was supported by the Deutsche Forschungsgemeinschaft within the Research Group BioGeoChemistry of the Wadden Sea (FG 432-TP5).

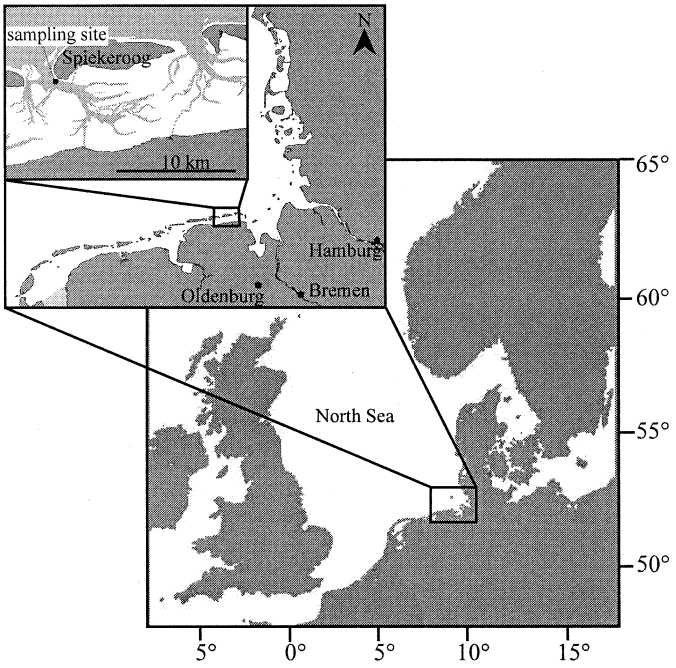

Fig. 1. Map of the study area and sampling site.

In tidal flat systems, the specific role and significance of bacteria in aggregate dynamics and in the decomposition of particulate organic matter (POM) has been neglected despite the generally important role of heterotrophic bacteria in organic matter decomposition in these systems. We hypothesize that in tidal flat ecosystems, bacteria are also important in the turnover of organic matter bound in aggregates and thus in aggregate dynamics.

The aim of this study was to investigate tidal and seasonal dynamics of microaggregates in a tidal flat ecosystem, the German Wadden Sea, and how their biological properties and physical forcing, i.e., the current velocity, affect these dynamics. The Wadden Sea, the coastal region of the North Sea between Den Helder (Netherlands) and Esbjerg (Denmark), is the largest tidal flat ecosystem globally and of general importance for land–sea interactions of the North Sea. We assessed SPM, its composition, and the aggregate size distribution and biochemical properties of various aggregate fractions, separated by their differential settling velocity. In addition, the abundance of aggregate-associated (AGG) and free-living (FL) bacteria, concentrations of dissolved amino acids, and DOC were assessed. To study the properties of different aggregate fractions was only possible by applying a newly developed sampling device that simultaneously served as a settling chamber (Lunau et al. 2004).

Materials and methods

Study site and sampling—Samples were collected on shipboard RV *Senckenberg* in the German Wadden Sea in the major tidal channel of the back-barrier area of the island Spiekeroog (Otzumer Balje, 53°44.9′N, 07°40.0′E, Fig. 1). Total water depth at the sampling site is ~15 m at high tide. The tidal range from high tide to low tide is ~ 2.8 m. Samples were collected at a fixed station by bucket from the surface or by a 10 L-horizontal sampling device (15 × 15 × 45 cm, Lunau et al. 2004) at 0.5–1 m depth over at least half a tidal cycle and up to two tidal cycles between January 2002 and October 2004, covering all important seasonal situations (Table 1). The sampling device ensured a careful collection of the aggregated suspended matter (SPM), minimizing a modification of the ambient aggregate size distribution. It allows a reliable documentation of the aggregate abundance and size distribution and serves as a settling chamber from which various fractions can be withdrawn for further analyses (see following). Seven samples were taken between the two slack water situations, thus subdividing this period into six equal time slots. The exact sampling time was derived from a hydrographical model for the German Bight and the adjacent Wadden Sea (Bundesamt für Seeschiffahrt und Hydrographie, Hamburg, Germany) and water-level recordings from a measuring pole (University of Oldenburg, http://las.physik.uni-oldenburg.de/wattstation/) located directly at the sampling station. Subsamples were withdrawn from the bucket immediately and from the sampling device after a settling time of 45 min and further processed within 10 min.

Documentation of aggregate abundance and size—Immediately after the sampling device was retrieved, it was turned into a vertical position, illuminated by a red light diode laser (λ = 658 nm, 50 mW), and the abundance and size distribution of the aggregates were documented by digital photography using a Sony Cybershot DSC-S70 (2002 and 2003) or Cybershot DSC-F828 (2004). The lower resolution of the DSC-S70 is 25 μm per pixel and that of the DSC-F828 is 15 μm per pixel. Further data processing and image analysis was done in the lab using the software package analySIS V 3.0 (Soft Imaging System, Muenster, Germany). We determined abundance, size distribution, equivalent circular diameter (ECD), and surface area of the aggregates. The surface area of aggregates was calculated assuming fractal geometry and D_2 as 1.6 and 1.8 for the growing season (Jun–Oct) and winter (Jan, Feb), respectively (Chen and Eisma 1995). For further details of the procedures of data analysis and the sampling device, see Lunau et al. (2004). To be sure that aggregate properties taken by the sampling device were not affected by handling artifacts, we compared the data from July 2003 with data from July 2005 taken by a recently developed in situ camera system over a semi-tidal cycle. It turned out that aggregate size, number, and dynamics were fairly similar, despite the interannual variability.

Sample fractionation—The vertically positioned sampling device allowed the aggregates to settle according to their density and settling behavior. After a settling time of 45 min, which is roughly the time of low-current velocities, i.e., <0.05 m s^{-1}, during slack water, subsamples for further analyses were withdrawn from the upper 15 cm (top), the central 15 cm (middle), the lower 15 cm (bottom), and the completely settled fraction (sediment). Here, we report only results from the top and sediment fractions, representing the

persistently suspended and the most rapidly sinking and least resuspended fractions.

Suspended particulate matter (SPM)—Subsamples of 500–1,000 mL were filtered onto precombusted (2 h, 450°C) and preweighed GF/F filters (Whatman, 47 mm diameter). Filters in 2003 and 2004 were rinsed with 10–20 mL of distilled water to remove salt and kept frozen at −20°C until further analysis in the lab within one week. Filters from 2002 were not rinsed but corrected for salt by linear regression analysis obtained from the comparison of a set of rinsed and unrinsed filters from 2003 (rinsed SPM = 0.9256 × unrinsed SPM − 16.492, $r^2 = 0.96$). After drying for 12 h at 60°C, filters were adapted to room temperature for 30 min and weighed again. SPM was calculated as the difference between filter weight before and after sample filtration and normalized per liter.

Particulate organic carbon (POC) and total particulate nitrogen (TPN)—Subsamples of 100 mL were filtered onto precombusted and preweighed GF/F filters (Whatman, 25 mm diameter), rinsed with 2–5 mL of distilled water to remove salt, and kept frozen at −20°C until further analysis. Prior to analysis the filters were exposed to the fume of concentrated hydrochloric acid for 12 h to remove carbonates. Thereafter, filters were folded, transferred into tin capsules (IVA, Meerbusch, Germany), and analyzed for POC and TPN by a FlashEA 1112 CHN-analyzer (Thermo Finnigan). Analysis was done at a combustion temperature of 1,000°C and a column temperature of 35°C. Concentrations were calculated by an external calibration curve with Methionin (0.1–2.5 mg).

Chlorophyll a (Chl a)—Subsamples of 500 mL were filtered onto GF/F filters (Whatman, 47 mm diameter), immediately wrapped into aluminum foil, and kept frozen at −20°C until further analysis in the shaded lab within one week. Filters were mechanically hackled and extracted in hot ethanol (75°C) for 1 h in the dark. Concentrations of Chl *a* were determined spectrophotometrically and calculated according to von Tuempling and Friedrich (1999).

Bacterial cell counts—Subsamples were filled into brown 50-mL glass bottles onboard ship, preserved with 2% (final concentration) Formaldehyde in 2002 and 2003 and with 2% (final concentration) glutardialdehyde in 2004, and stored at 4°C in the dark until further processing. In 2002, the total sum of free-living and aggregate-associated bacteria (Bac) were enumerated after DAPI staining by epifluorescence microscopy (Porter and Feig 1980). In 2003 and 2004, abundances of total bacteria, FL bacteria, and AGG bacteria were enumerated after staining with SybrGreen I by epifluorescence microscopy, applying a new detachment procedure. For FL bacteria, the sample was centrifuged (RCF = 380 g) to separate bacteria from other particulates and a 500 to 1,000 μL subsample of the supernatant after centrifugation was filtered through a black 0.2 μm polycarbonate filter (Poretics, 25 mm diameter, shiny side up). Cells were washed with 3–5 mL of a TAE-methanol mix (1 : 1, pH 7.4), the filter transferred to a microscope slide and stained by SybrGreen I mixed into the mounting solution (1 : 40) containing moviol 4–88 (polyvinylalcohol 4–88). For the determination of Bac, the sample was treated with 10–30% methanol (35°C) and ultrasonication before centrifugation. The number of AGG bacteria was calculated as the difference of Bac minus FL bacteria. This procedure is particularly suitable for samples with high loads of SPM and results in a very efficient detachment of AGG bacteria, yielding reliable numbers of the latter with a standard error of <15%. For further details of the method, see Lunau et al. (2005).

Stained cells were counted with a Zeiss Axiolab 2 microscope at 1,000× magnification by using a 100× Plan-Apochromat oil-immersion objective (lamp: HBO 50, filter set: Zeiss, Ex 450–490, FT 510, LP 515). The filtered sample volume yielded 60–150 stained cells in the counting grid. For each sample, 10 grids and a minimum of 600 cells per filter were enumerated.

Bacterial production (BP)—Rates of BP, measured only during the tidal cycles in June and October 2004, were determined by the incorporation of ^{14}C-leucine (Simon and Azam 1989). Triplicates and a formalin-killed control were incubated with ^{14}C-leucine (10.8 GBq mmol^{-1}, Hartmann Analytic, Germany) at a final concentration of 70 nmol L^{-1}, which ensured saturation of uptake systems. Incubation was performed in 10-mL plastic test tubes in the dark at in situ temperature for 1 h on a plankton wheel to avoid sedimentation. After fixation with 2% formalin, samples were filtered onto 0.45 μm nitrocellulose filters (Sartorius, Germany) and extracted with ice-cold 5% trichloroacetic acid (TCA) for 5 min. Thereafter, filters were rinsed twice with ice-cold 5% TCA, dissolved with ethylacetate, and radio-assayed by liquid scintillation counting. Biomass production was calculated according to Simon and Azam (1989). Standard deviation of triplicate measurements was usually <15%.

Amino acid analysis—Concentration of dissolved free (DFAA), total hydrolyzable dissolved (THDAA), and total hydrolyzable amino acids (THAA) were analyzed by high-performance liquid chromatography (HPLC) after orthophthaldialdehyde precolumn derivatization (Lindroth and Mopper 1979). An Alltima reverse phase column (C-18, 5 μm, 250 mm, Alltech) was used in combination with an Allguard (Alltech, Germany) precolumn. Subsamples for DFAA and THDAA were filtered on board through 0.2 μm low-protein-binding filters (Tuffrin Acrodisc, Pall) and kept frozen at −20°C until analysis. DFAA were measured directly after addition of α-amino butyric acid (α-ABA) at a concentration of 40 nmol L^{-1} as an internal standard.

THDAA and THAA were analyzed as DFAA after hydrolysis in 6 N HCl (final conc.: 1.7 and 2.3 mol L^{-1}) at 155°C for 1 h in glass ampoules, sealed under nitrogen gas. Prior to analysis, the internal standard (α-ABA, 40 nmol L^{-1} final concentration) and ascorbic acid (40 μg mL^{-1} final concentration), to prevent oxidation of the amino acids by nitrate, were added to the sample. Prior to analysis, THDAA and THAA samples were diluted by ultrapure water (Seralpur) 1 : 10 and 1 : 25, respectively. The concentration of dissolved combined amino acids (DCAA) was calculated as the difference of THDAA minus DFAA and the concentration of

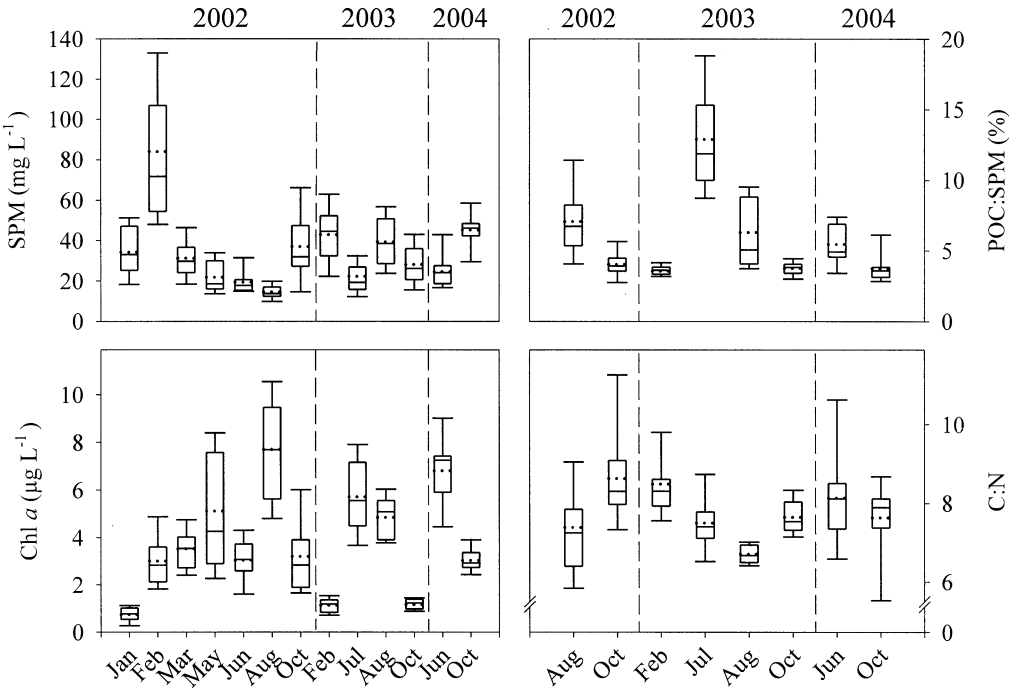

Fig. 2. Seasonal dynamics of suspended particulate matter (SPM), Chlorophyll *a* (Chl *a*), particulate organic carbon over SPM (POC : SPM), and the C : N ratio. Box-Whisker-Plots show the tidal means (dotted line) and median (solid line). Error bars indicate the 5 and 95 percentiles and the boxes the 25 and 75 percentiles.

particulate combined amino acids (PCAA) as the difference of THAA minus THDAA.

Dissolved organic carbon (DOC)—Subsamples of 50 mL were filtered through precombusted GF/F filters on board ship. The filtrate was stored at 4°C in brown glass bottles after acidification to pH 2 by HCl until analysis within one week. DOC concentrations were determined after high temperature oxidation by a multi N/C 3000 analyzer (Analytik Jena, Germany). Potassium hydrogen phthalate was used as external standard.

Results

Thirteen tidal events were investigated, of which 8 were sampled for roughly 2 entire tidal cycles, 2 for half a cycle, and 3 for various periods between 1 and 1.5 cycles (Table 1). The tidal events included spring tides as well as neap tides but also various situations in between. In situ temperature ranged from −0.2°C in January to 26°C in July, and salinity from 26 to 32, respectively, with only minor tidal variations. The current velocity maximum around mean tide varied 1.5–1.8 m s^{-1}. All properties assessed exhibited great variations, seasonally, over a tidal cycle, but also interannually, and tidal variations were often as high as the range of the tidal means over the seasonal situations (Table 1, Fig. 2). We note that, except for SPM and Chl *a*, properties were not assessed during all tidal events studied.

SPM and POC concentrations ranged 10–70 mg L^{-1} and ~0.5–~4 mg L^{-1}, respectively, except for a situation in February 2002, when a heavy storm caused strong resuspension, raising SPM concentrations up to 173 mg L^{-1} (Table 1, Fig. 2). Aggregate abundance was highly variable. Highest numbers occurred in October 2004 and lowest numbers in July and August 2003 (Table 1). The aggregate size (ECD) ranged between 82 and 112 μm (tidal means), but variations during tidal cycles were higher than seasonally and interannually (Table 1). The rather high numbers of aggregates and low ECD values of the tidal cycles in June and October 2004 are due to the application of the new camera with a higher resolution as compared to the previous years. Concentrations of Chl *a* also varied greatly with elevated values from May to August (Table 1, Fig. 2). Variations of the C : N ratio were higher tidally than seasonally and interannually, indicating pronounced differences in the composition of the suspended POM during tidal cycles (Table 1). DOC concentrations, ranging between ~130 and ~445 μmol C L^{-1}, were highly variable during tidal cycles, exceeding variations of the tidal means seasonally and interannually (Table 1). Concentrations of DFAA also varied greatly with highest values and tidal amplitudes in June and August 2003 (Table 1). Serine, glycine, tyrosine, and valine constituted the highest proportions of DFAA, comprising 20–30, 10–30, 10–15, and 5–15 mol%, respectively. Mol% remained unchanged tidally and did not show any clear seasonal trend. Concentrations of DCAA were not much higher than those of DFAA, but tidal and seasonal variations showed different patterns (Table 1). Serine, glycine, glutamate, tyrosine, and aspartate were the most abundant amino acids and constituted 18–23, 16–20, 10–15, ~10, and 5–12 mol%, respectively, and did not show any clear seasonal trend. Concentrations of PCAA were substantially higher than those of DCAA, ranging 3.4–7.4 μm as tidal means, and tidal amplitudes were rather similar (except in Feb 2002) at the storm event (Table 1). Num-

bers of FL bacteria varied tidally as well as seasonally and interannually with elevated values in June, July, and August as compared to other periods (Table 1). Numbers of AGG bacteria per mL varied less than those of FL bacteria and remained rather similar (Table 1). AGG bacteria constituted 23–50% of total bacteria with highest proportions in February. Numbers of AGG bacteria normalized per mg SPM varied even more with lower numbers in October and February and substantially higher numbers from May to August (Table 1). Numbers were also highly variable during the tidal cycles.

Normalized tidal cycle—To identify systematic and recurrent patterns and relationships in the tidal dynamics of the various properties (irrespective of the seasonal and interanual variabilities), we developed an empirical model of the typical tidal dynamics of each property assessed (Formula 1). Therefore, we normalized all values of a given property of one tidal cycle as percent of its tidal mean and calculated the means of these numbers for the data set of the tidal cycles of 2002 and 2003 available for each property:

$$\frac{1}{N_1}\sum_{i=1}^{N_1}\left(\frac{x_{i,t}}{\frac{1}{N_2}\sum_{t'=1}^{N_2}x_{i,t'}}\cdot 100\right)=\bar{X}_t \qquad \text{Formula 1}$$

N_1 = Number of cruises, N_2 = Number of samples during a particular cruise, $x_{i,t}$ = absolute value x of a property sampled during cruise i at a specific tidal phase t, $x_{i,t}'$ = absolute value x of a property sampled at time t' during the particular cruise i, X_t = averaged normalized property value at a specific tidal phase, based on the proportion of the absolute measurement values to its tidal mean in %.

The mean variation of the individual data points from the calculated mean at each sampling point was ~30%. Prior to this calculation and because the various investigations started at different tidal phases, the tidal cycles were reordered such that the start of each was set at low tide (LT) late at night. The current velocity data, treated in the same way as the other measurements, were derived from a hydrographic model of the backbarrier tidal flat system (Stanev et al. 2003), taking into account the various biweekly phases from spring to neap tide (Table 1).

This general model yielded typical tidal patterns of all properties characterizing the particulate material and showing their control by the tidal currents. The CVM during incoming tide was lower than during outgoing tide and appeared 3–4 h after slack water during the flood tide as compared to 2 h after slack water during ebb tide (Fig. 3A, B). Thus, the slack-water period was significantly shorter around high tide (HT) as compared to LT. This asymmetric current pattern is a result of the specific morphometry of this backbarrier system (Stanev et al. 2003). Cross-correlation analysis showed that the dynamics of SPM and POC generally covaried with the current velocity patterns by a time lag of 1 h (SPM: $r^2 = 0.65$, POC: $r^2 = 0.55$), but maxima were higher during incoming tide as compared to outgoing tide and occurred 4 h after slack water, 1–2 h after the CVM (Fig. 3C,E,G,I). Minima occurred 1 h after slack water and were systematically higher at HT in the morning as compared to the other slack-water situations. Minima at HT in the morning were least pronounced with POC and Chl *a*. The C : N ratio was higher around slack water as compared to phases of enhanced current velocities and particularly high around HT in the early night (Fig. 3H). ECD of aggregates was largest around slack water and decreased rapidly at the CVM 2 h after HT (Fig. 3K). It decreased less during outgoing tide with a lower CVM. DOC concentrations gradually increased from HT to 1–2 h after LT with an intermediate peak 2 h after HT (Fig. 3D). Total bacterial numbers exhibited maxima 2–4 h after slack water (Fig. 3F). Minima were lowest at HT.

The various properties exhibited pronounced differences with respect to the deviations from the mean. Whereas the current velocity varied from 10% to 190% of its mean, variations of SPM, POC, and Chl *a* ranged from ~60% to 140%. The aggregate abundance varied more, 30–180%, and DOC, total bacterial numbers, C : N and the ECD much less.

The various properties characterizing the SPM and normalized to the typical tidal cycle were positively correlated to each other (Table 2). AGG abundance was also positively correlated to the current velocity, whereas the ECD was inversely correlated to the current and the water level. Bacteria and DOC were not correlated to properties characterizing the particulate phase but negatively to the water level and positively to each other.

Aggregate size distribution—To examine the tidal dynamics of the aggregates' size distribution, we compared the abundance and surface area of aggregate size classes 38–511 μm (mean ECD) at HT, mean tide (MT), and LT of two contrasting tidal cycles, of February and July 2003 (Fig. 4). Aggregate abundance and surface area in February were roughly tenfold higher than in July, but the mean size of aggregates (tidal means of ECD) in July was 15% larger than in February. Highest proportions of aggregates occurred in the smallest size fractions at MT, but in July, the size range was skewed towards larger size classes. At this tidal event, the relative abundances in the various size classes at HT and LT were rather similar, whereas in February, they were higher at HT than at LT. The surface area of each size class remained below 0.5×10^3 mm^2 in July with highest values at MT and much lower and rather similar values at HT and LT. In contrast, in February, the surface area of each size class was substantially greater, reaching $1.3–4 \times 10^3$, $0.8–2.5 \times 10^3$, and $0.4–1 \times 10^3$ mm^2 in the size classes 38–262 μm at MT, HT, and LT, respectively.

Geochemical and microbial properties of aggregate fractions separated by differential settling—To further examine properties of the various aggregate fractions during tidal cycles and seasonally, we separated aggregates by their different settling rates using the new sampling device and collected them for subsequent chemical and microbial analyses. Here, we present results from 2 tidal cycles of June and October 2004, differing in particular in concentrations of SPM and Chl *a* (Figs. 2, 5). We focused on the aggregate fraction remaining suspended in the upper 15 cm of the settling chamber after 45 min (Top) and that settling completely to its bottom (Sed). These fractions exhibit pronounced dif-

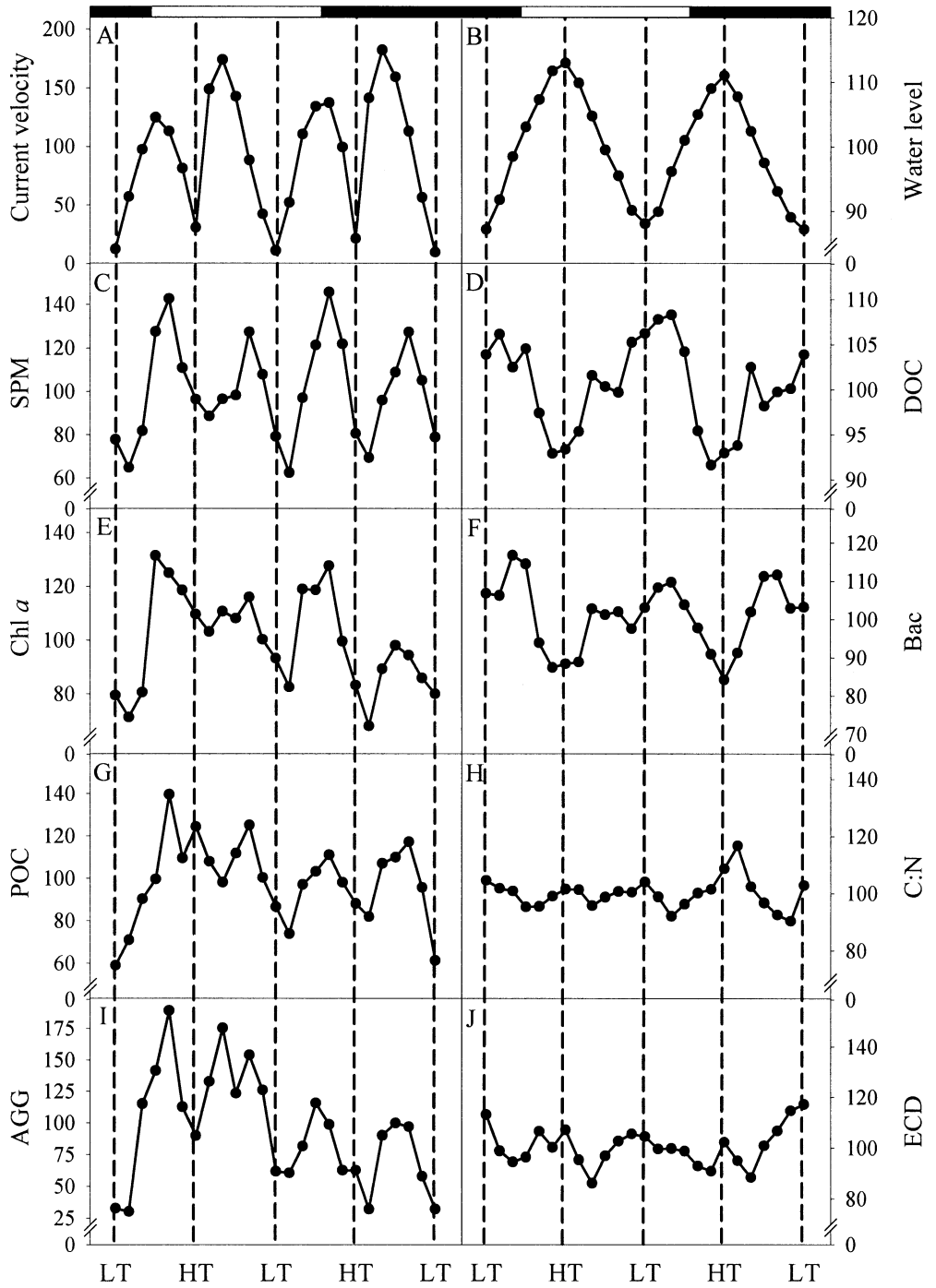

Fig. 3. Patterns of the current velocity, water level, SPM, DOC, Chl *a*, bacterial numbers (Bac), POC, C : N ratio, aggregate abundance (AGG), and the aggregate equivalent circle diameter (ECD) of two consecutive tidal cycles. The data of one tidal cycle were normalized as percent of its tidal mean and the means of these numbers were calculated for the data set of the tidal cycles of 2002 and 2003 available for each property (for details see Formula 1). Prior to this calculation the tidal cycles were reordered such that the start of each was set at low tide late at night. LT: Low tide; HT: High tide. The black and white bars on top indicate night and day periods.

ferences among each other and as compared to the bulk sample (in situ) between the 2 tidal cycles, but also at different phases within one cycle.

The Top layer of the settling chamber was deprived of (Jun: $p = 0.01$; Oct: $p < 0.01$, *t*-tests) and the Sed fraction substantially enriched (Jun: $p < 0.001$; Oct: $p = 0.002$, Mann-Whitney-test) in SPM as compared to the bulk sample (Fig. 5A,B). Differences between the bulk sample, the Top fraction, and the Sed fraction were generally greater in October (difference of ranks: Bulk vs. Top = 23, Sed vs. Bulk = 334, Sed vs. Top = 357, Tukey-test) than in June (Bulk vs. Top = 7, Sed vs. Bulk = 7, Sed vs. Top = 14). However,

Table 1. Means, minima, and maxima of SPM, POC, Chl *a*, C : N-ratio, DOC, aggregate abundance (AGG), equivalent circle diameter (ECD), concentrations of DFAA, DCAA, and PCAA, numbers of total bacteria (Bac), free-living (FL), and aggregate-associated bacteria (AGG Bac) of all tidal cycles studied in 2002, 2003, and 2004. The frequency of sampling during one tidal event (*n*) and the days to new moon (NM) are given.

Date	*n*	days to NM	SPM (mg L^{-1})		POC (mg L^{-1})		Chl *a* (μg L^{-1})		C : N		DOC (μmol L^{-1})	
			mean	min max	mean	min max	mean	min max	mean	min max	mean	min max
08–09 Jan 02	22	5	34.4	14.6–54.0	—	—	0.7	0.2–1.1	—	—	—	—
06–07 Feb 02	26	6	84.0	43.7–173.0	—	—	3.0	1.4–5.4	—	—	237.4	188.2–290.2
26–27 Mar 02	23	17	31.3	17.1–51.2	—	—	3.5	1.9–5.0	—	—	—	—
07–08 May 02	26	5	21.9	12.5–35.7	—	—	5.1	1.7–8.6	—	—	—	—
03–04 Jun 02	17	8	19.4	14.6–35.5	—	—	3.1	1.4–5.0	—	—	—	—
06–07 Aug 02	25	2	14.6	8.6–21.4	1.0	0.4–1.8	7.7	2.6–12.7	7.4	5.5–13.0	211.9	173.2–252.3
07–08 Oct 02	25	16	37.1	12.2–72,6	1.4	0.7–2.5	3.2	1.3–6.9	8.6	7.2–11.3	210.8	183.2–252.3
17–18 Feb 03	25	14	43.0	18.4–68.0	1.5	0.3–2.4	1.1	0.6–1.8	8.5	7.3–11.1	—	—
22–23 Jul 03	25	6	22.3	9.8–57.3	2.6	1.7–5.4	5.7	2.6–8.1	7.5	5.7–9.6	—	—
27–28 Aug 03	19	0	39.4	22.6–65.6	2.4	1.1–4.2	4.8	2.7–6.2	6.7	6.4–7.1	196.8	175.7–228.4
28 Oct 03	13	15	28.2	14.1–43.3	1.0	0.6–1.7	1.2	0.8–1.5	7.6	7.1–8.4	201.1	184.2–236.7
08 Jun 04	9	10	24.7	16.8–43.0	1.3	0.9–1.9	6.8	4.5–9.0	8.1	6.6–10.6	344.6	270.0–445.8
20 Oct 04	7	13	45.8	29.6–58.6	1.7	1.1–2.6	3.1	2.4–3.9	7.6	5.4–8.7	166.3	131.8–192.0

Date	*n*	days to NM	AGG ($\times 10^3$ mL^{-1})		ECD (μm)		DFAA (μmol L^{-1})		DCAA (μmol L^{-1})		PCAA (μmol L^{-1})	
			mean	min max	mean	min max	mean	min max	mean	min max	mean	min max
17–18 Feb 03	25	14	0.5	0.06–2.4	87.8	64.4–110.3	0.5	0.1–1.3	0.6	0.2–2.1	6.3	2.2–23.7
22–23 Jul 03	25	6	0.2	0.05–0.5	101.5	80.6–133.9	0.8	0.1–3.0	0.8	0.4–1.6	3.6	1.8–7.1
27–28 Aug 03	19	0	0.3	0.08–0.4	111.8	74.8–137.5	1.0	0.5–1.7	1.7	1.2–2.3	7.4	5.0–10.6
28 Oct 03	13	15	1.1	0.10–1.9	101.4	76.8–128.0	—	—	—	—	—	—
08 Jun 04	9	10	1.3	0.34–2.7	82.1	71.2–87.1	0.3	0.1–0.7	1.3	0.9–1.7	7.6	5.4–10.2
20 Oct 04	7	13	4.0	1.00–10.4	92.7	61.9–121.3	0.2	0.1–0.7	1.7	1.3–2.7	3.4	2.6–5.4

Date	*n*	days to NM	Bac ($\times 10^6$ mL^{-1})		FL bacteria ($\times 10^6$ mL^{-1})		AGG bacteria ($\times 10^6$ mL^{-1})		AGG bacteria ($\times 10^6$ (mg SPM)$^{-1}$)	
			mean	min max	mean	min max	mean	min max	mean	min max
07–08 May 02	26	5	3.9	2.7–4.9	—	—	—	—	—	—
03–04 Jun 02	17	8	6.0	3.0–7.5	—	—	—	—	—	—
06–07 Jul 02	25	2	7.2	4.6–9.3	—	—	—	—	—	—
07–08 Oct 02	25	16	4.8	4.2–5.9	—	—	—	—	—	—
17–18 Feb 03	5	14	0.8	0.7–1.0	0.4	0.3–0.5	0.4	0.2–0.8	9.6	3.4–19.3
22–23 Jul 03	25	6	2.5	0.4–2.9	1.7	1.4–2.1	0.8	0.5–1.3	40.8	16.8–85.3
27–28 Aug 03	19	0	2.7	2.0–3.4	1.9	1.3–2.6	0.8	0.3–0.9	23.3	2.8–49.2
28 Oct 03	5	15	1.1	1.0–1.3	0.8	0.7–0.9	0.4	0.2–0.5	16.9	6.8–22.0
08 Jun 04	9	10	3.9	3.1–4.3	3.0	2.2–3.6	0.9	0.6–1.6	38.8	16.3–67.7
20 Oct 04	7	13	1.8	1.3–2.4	1.2	0.8–1.4	0.7	0.3–1.2	14.7	6.9–25.2

Table 2. Correlation analysis of SPM, POC, Chl *a*, DOC, water level, current velocity (Cur Vel), aggregate abundance (AGG), C : N ratio, numbers of total bacteria (Bac), and the equivalent circle diameter (ECD) of tidal dynamics. Given is the correlation coefficient of the Pearson-Product-Moment analysis based on the normalized data shown in Fig. 3. *p*-values are in italic and significant correlations are in bold. $n = 25$ for all properties.

	POC	Chl *a*	C : N	DOC	AGG	ECD	Bac	Cur Vel	Wat Lev
SPM	**0.758**	**0.797**	**−0.515**	−0.298	**0.625**	−0.080	−0.037	0.390	0.289
	<0.001	*<0.001*	*<0.001*	*0.149*	*<0.001*	*0.705*	*0.862*	*0.054*	*0.162*
POC		**0.706**	−0.395	−0.430	**0.756**	−0.197	−0.244	0.477	0.517
		<0.001	*0.050*	*0.032*	*<0.001*	*0.346*	*0.240*	*0.015*	*0.008*
Chl *a*			**−0.532**	−0.122	**0.743**	−0.216	−0.072	0.378	0.398
			0.006	*0.562*	*<0.001*	*0.299*	*0.734*	*0.062*	*0.048*
C : N				−0.317	−0.452	−0.113	−0.458	−0.214	0.213
				0.122	*0.023*	*0.590*	*0.021*	*0.303*	*0.307*
DOC					−0.093	0.159	**0.751**	−0.170	**−0.781**
					0.657	*0.447*	*<0.001*	*0.415*	*<0.001*
AGG						−0.325	<0.001	**0.519**	0.365
						0.113	*1.000*	*0.008*	*0.073*
ECD							0.0451	**−0.733**	**−0.526**
							0.830	*<0.001*	*0.007*
Bac								0.118	**−0.662**
								0.576	*<0.001*
Cur Vel									0.427
									0.033

tidal variations between both fractions were lower in October—except at slack water of LT (data at HT are not available)—reflecting a more conservative behavior of both fractions. These differences were also reflected in the ratio POC : SPM, which was generally higher in June than in October (ANOVA, $p = <0.001$), and also higher in the Top fraction than the Sed fraction (Jun: $p = 0.004$; Oct: $p < 0.001$, *t*-tests; Fig. 5C,D). Highest ratios were recorded in June in the Top fraction around HT and in the Sed fraction 1 h before LT, following the maxima in concentrations of SPM and POC in the bulk sample by 1 h. The former maximum reflected the persistence of POC-rich aggregates in suspension and sedimentation of POC-rich material and the latter substantial POC sedimentation shortly before LT. The C : N ratios of the fractionated samples were significantly different in June and October ($p = 0.003$, ANOVA). In June, the C :

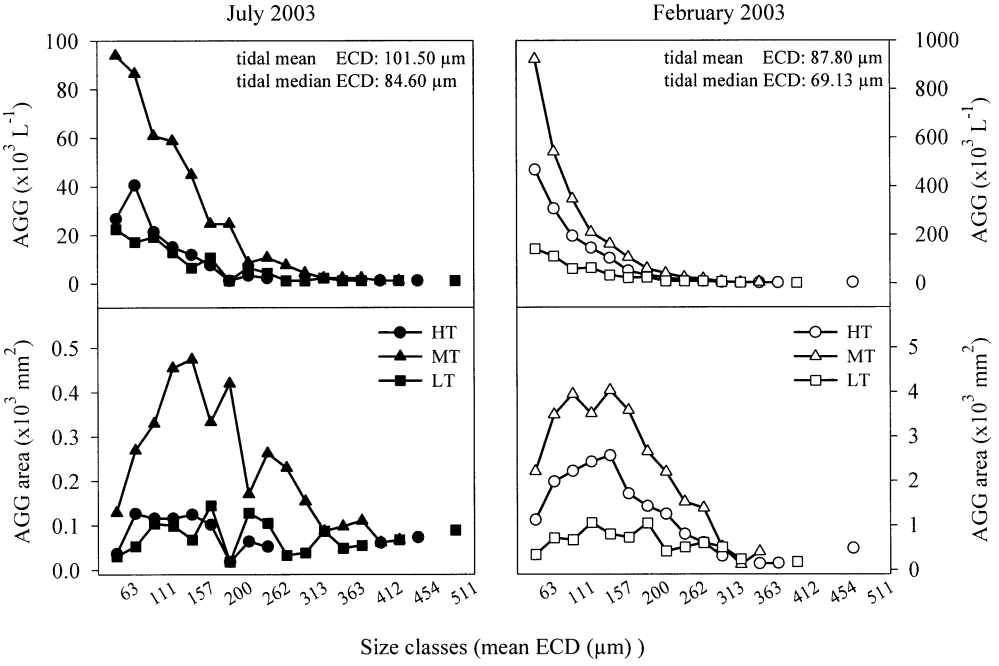

Fig. 4. Abundance and surface area of aggregates in the size classes 35–511 μm at HT, MT, and LT of semi-tidal cycles in July and February 2003 during day time. For abbreviations, *see* Fig. 3.

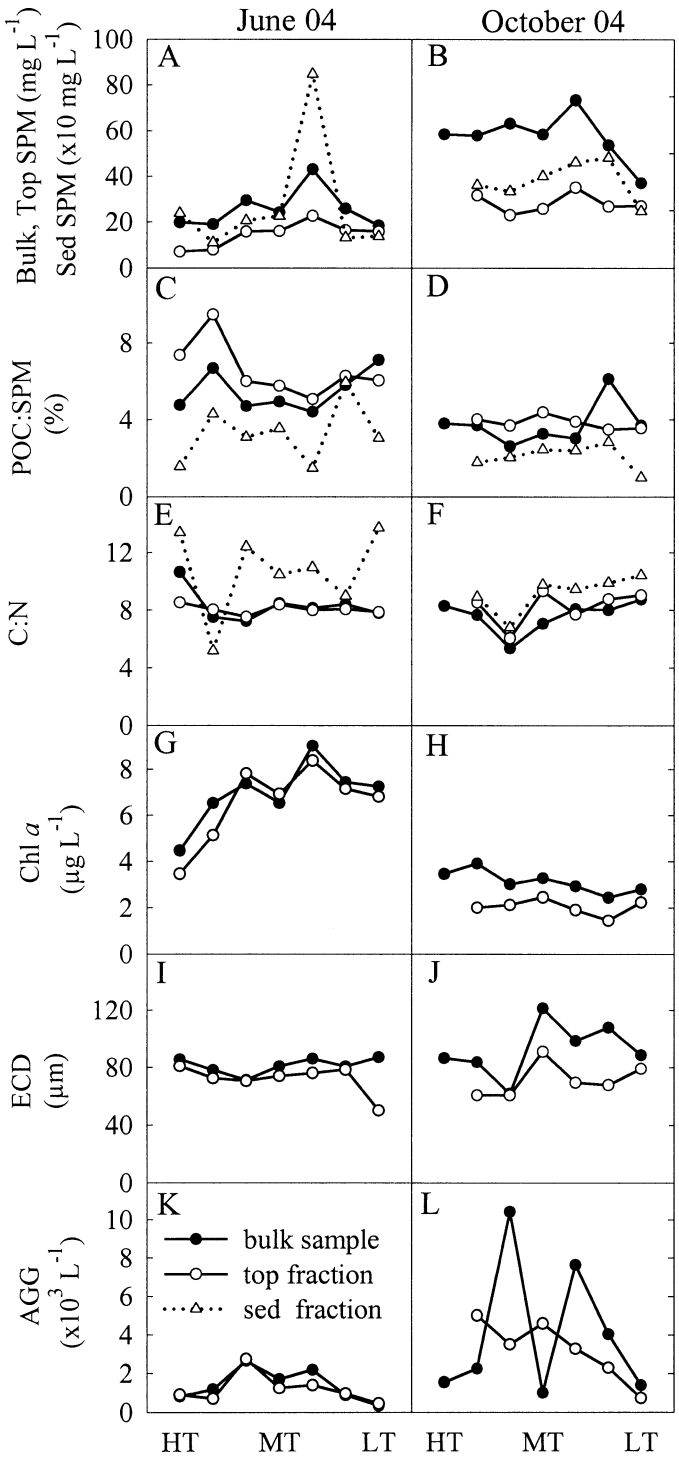

Fig. 5. SPM, POC : SPM, C : N ratio, Chl a, ECD, and aggregate abundance (AGG) of particulates of semi-tidal cycles at day time in June and October 2004. Given are the fraction remaining suspended at the top (Top fraction) of the settling chamber after 45 min and settled to its bottom (Sed fraction), and the bulk sample (in situ). Note the different scales of the y-axes of SPM in the Top and Sed fractions in panel A. MT: Mean tide, for other abbreviations *see* Fig. 3.

N ratio in the Sed fraction was substantially higher compared to the Top fraction and the bulk sample ($p < 0.05$, Tukey test), whereas in October, no significant difference between the bulk sample, the Top fraction, and the Sed fraction were observed. Concentrations of Chl *a* in the Top fraction did not differ significantly to the bulk sample but were substantially lower in October, at generally lower concentrations of Chl *a* ($p < 0.001$, ANOVA; Fig. 5G,H). Chl *a* was not determined in the Sed fraction.

Despite these differences in the properties of particulates in the Top and Sed fractions and as compared to the bulk sample, the tidal variations of aggregate abundance and size in the Top fraction and the bulk sample (Fig. 5I–L) did not differ significantly neither in June nor in October. But we assume the lower ECD of aggregates in the Top fraction at LT in June to indicate settling out of larger and POC-deprived aggregates. Because the Sed fraction was concentrated in a small receptacle, aggregate abundance and size could not be determined.

Numbers of FL and AGG bacteria in the bulk sample, the Top, and the Sed fraction were different from each other during both tidal cycles ($p < 0.001$, ANOVA; Fig. 6A–D). Separate analyses of FL and AGG bacteria for the particular month showed that there was no significant difference between the FL bacteria in the three fractions in June ($p = 0.19$), which is probable due to the pronounced dynamics of this bacterial fraction throughout the tidal cycle. Furthermore, the numbers of FL bacteria in the Top fraction increased and in the Sed fraction decreased from 1 h after HT to 1 h after MT, whereas in the bulk sample they only strongly increased from MT to 1 h later, similarly with SPM, POC, and Chl *a* (Fig. 5C,E,G). In October, the number of FL bacteria in the Top fraction differed significantly from the bulk sample and the Sed fraction ($p < 0.001$ rsp. $p = 0.002$, Tukey test). Numbers of AGG bacteria, normalized per mg SPM, were always higher in the Top fraction than in the Sed fraction ($p < 0.05$, ANOVA), and yielded lower numbers in the Sed fraction compared to the bulk sample in October ($p < 0.05$, ANOVA). In June in the Top fraction, they decreased from HT to LT with the strongest drop from HT to 1 h later, simultaneously with the increase in numbers of FL bacteria. In the Sed fraction, peaks were recorded 1 h after HT and 1 h before LT, simultaneously with peaks in the ratio POC : SPM (Fig. 5C). In October, there was also an inverse covariation of numbers of FL and AGG bacteria, but less pronounced than in June. Numbers of AGG bacteria in the Sed fraction remained unchanged tidally. Rates of BP, measured only of the total bacterial community, exhibited pronounced differences between the 2 fractions and the bulk sample in October ($p < 0.001$, ANOVA), when it remained generally low with little tidal dynamics (Fig. 6E,F), but less significant in June ($p = 0.046$, ANOVA, compare with FL bacteria above). In June, BP rates in the bulk sample were high after HT and around LT, together with enhanced ratios of POC : SPM (Fig. 5C). In the Top fraction, enhanced BP rates followed those in the bulk sample by 1 h. In October, the rates were higher than in the Top fraction and the bulk sample ($p = 0.002$ rsp. $p = 0.004$, Tukey test), despite lower numbers of AGG bacteria in this fraction (Fig. 6D).

Concentrations of dissolved amino acids exhibited sub-

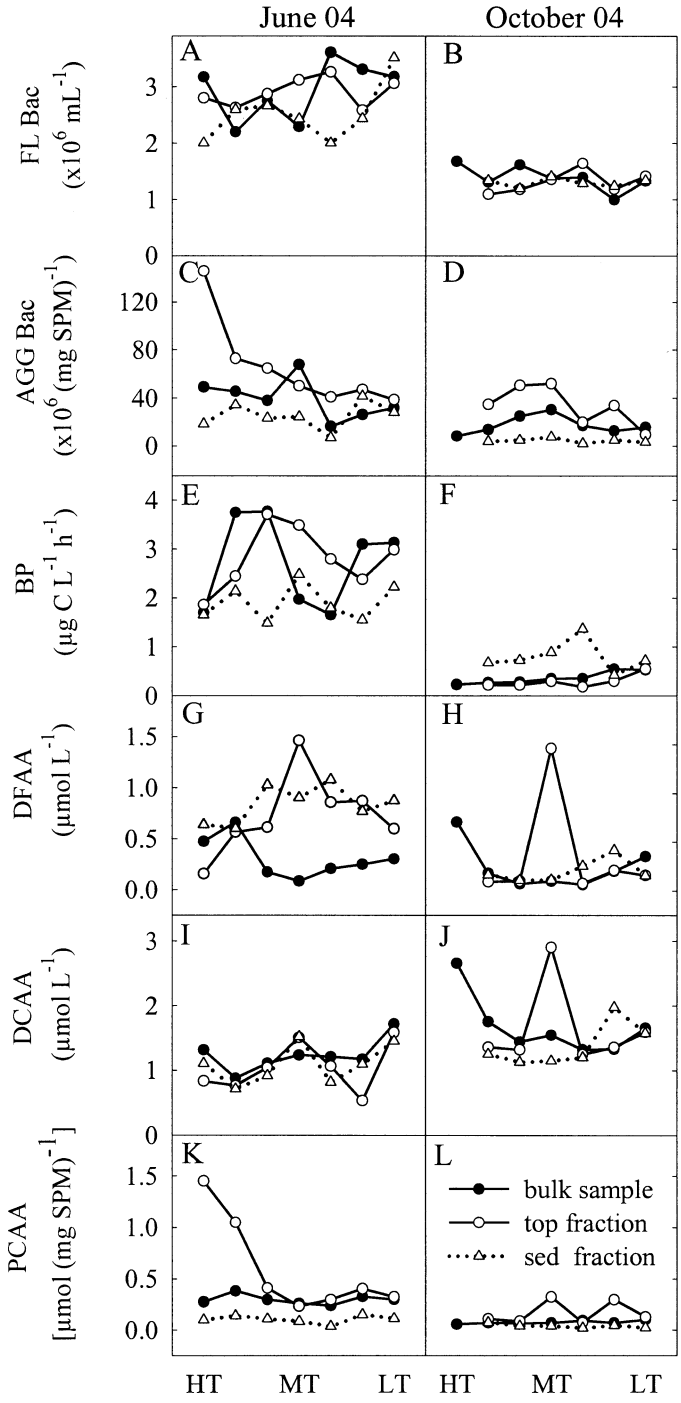

Fig. 6. Numbers of free living (FL Bac) and aggregate-associated bacteria (AGG Bac), bacterial biomass production (BP), and concentrations of DFAA, DCAA, and PCAA of particulates of semi-tidal cycles at day time in June and October 2004. Given are the fraction remaining at the top (Top fraction) of the settling chamber after 45 min and at its bottom (Sed fraction), and the bulk sample (in situ). MT: Mean tide, for other abbreviations *see* Fig. 3.

stantial variations during both tidal events (Fig. 6G–J). In June, DFAA and DCAA concentrations in both fractions increased towards MT and decreased thereafter, but these patterns were not recorded in the bulk sample. At slack water, DCAA concentrations were elevated as well. DFAA concentrations in the Top, and the Sed fraction were substantially higher than in the bulk sample ($p = 0.028$ resp. $p = 0.006$, Tukey test), but DCAA concentrations were rather similar ($p > 0.05$, ANOVA). In October, there were only little differences between the concentrations of DFAA ($p = 0.816$, Kruskal-Wallis) and DCAA ($p = 0.212$, Kruskal-Wallis) of both fractions, except at MT when a pronounced peak in DFAA concentrations occurred, similar to June. PCAA concentrations, normalized to mg SPM, exhibited much less variability (Fig. 6K,L). In June, PCAA concentrations in the Sed fractions were lower than in the other fractions ($p < 0.05$, Tukey test), and the top fraction was highly enriched in PCAA around HT, simultaneously with enhanced ratios of POC : SPM (Fig. 5C). In October, the Top fraction was enriched in PCAA compared to the bulk sample and the Sed fraction ($p < 0.05$, Tukey test), while the latter ones showed no significant difference ($p > 0.05$, Tukey test).

Discussion

The significance and dynamics of SPM and aggregates and processes of aggregation in turbid and shallow tidally affected systems, such as tidal flats and estuaries, have been studied extensively for more than a decade. A major focus of the studies in these systems, in which SPM is largely dominated by inorganic matter, has been on hydrodynamic aspects of aggregation, including the flow field, turbulence, collision frequency, shear, settling, and fractal geometry (Lynch et al. 1994; ten Brinke 1994; Milligan 1995). These studies have shown that the current velocity, SPM and aggregate concentrations are positively correlated, resulting in high sinking rates at low and intense resuspension at high current velocities, and that the aggregate size is inversely correlated to the latter. On the other hand, the organic components of the SPM have been also characterized to their elemental (C, N) and biochemical constituents such as Chl *a*, protein, carbohydrates, and lipids (Mannino and Harvey 2000; Murrell and Hollibaugh 2000; McCandliss et al. 2002). There is limited information available that aggregate-associated bacteria exhibit high rates of biomass production and hydrolytic enzyme activities in turbid aquatic systems such as the estuarine turbidity maximum zone and tidal flats, indicating that bacteria are an active component for organic matter degradation (Plummer et al. 1987; Crump et al. 1998; Crump and Baross 2000). However, virtually no information is available on the elemental and biochemical composition and on the microbial colonization of specific aggregate fractions differing in size, density, and settling properties.

Reason for the lack of such information is that it is difficult to separate various aggregate fractions for subsequent analyses. Settling velocity tubes have been applied to separate various SPM fractions with respect to dry weight and Chl *a* near the surface and the bottom during tidal cycles in the southern North Sea, showing pronounced differences at both water layers and during varying energetic conditions (McCandliss et al. 2002). This device, however, is not suitable to analyze the size distribution of the various aggregate fractions. The application of the new sampling device, serv-

ing simultaneously as a settling chamber (Lunau et al. 2004), and of a new desorption and counting procedure for aggregate-associated bacteria (Lunau et al. 2005) enabled us to overcome these difficulties and to obtain reliable data on the size, elemental and biochemical composition, and the bacterial colonization of aggregate fractions differing in their settling properties. The settling time of 45 min, equivalent to the period of low current velocities around slack water, allowed the aggregate fraction with the lowest ratio POC : SPM to settle out such that an aggregate fraction with a higher ratio POC : SPM than the bulk sample remained suspended. These two fractions exhibited distinct differences with respect to the C : N ratio, PCAA, the bacterial colonization, and dynamics in the June and October tidal cycles, indicating that hydrodynamic forcing—i.e., collision frequency—shear, and differential settling resulted not only in restructuring the aggregate size distribution, but also in modifying their quality. In June, the C : N ratio, Chl *a*, aggregate size (ECD) and abundance of the Top fraction covaried more with the bulk sample than in October, indicating that this fraction, enriched in POC, PCAA, and harboring more bacteria than the Sed fraction, dominated bulk SPM. In contrast, in the October tidal cycle, which was more typical for a fall and winter situation with respect to enhanced SPM concentrations, reduced aggregate size, and a low bacterial colonization (Table 1), the Sed fraction dominated more the bulk sample. As shown previously, the settling chamber allows an even more detailed separation of aggregate fractions, differing in their settling rates but also in their ratios of dryweight:aggregate, POC:aggregate and C : N and exhibiting distinct tidal differences (Lunau et al. 2004).

The results of the settling chamber further show that intense microbial processes occur on and around the aggregates of the Top and Sed fractions within the settling time, resulting in detectable changes in the abundance of free-living and aggregate-associated bacteria, in bacterial production rates and concentrations of DFAA and DCAA as compared to the bulk sample and in the course of tidal cycles. Concentrations of DFAA and DCAA in the Top and Sed fraction were enhanced around MT in June, and distinct peaks occurred in the Top fraction at MT, 1 h after the CVM, both in June and October. These distinct peaks appeared surprising and we have no clear-cut explanation for them. Because they occurred in both tidal cycles we assume that they are no artifact but reflect intense DOM release processes from aggregates at this time of maxima of SPM, POC, and aggregate abundance (Fig. 3). These changes remain unnoticed when only collecting bulk samples. Considering these changes and the fact that aggregate-associated bacteria exhibit high ectoenzymatic hydrolytic activities, affect the aggregation of diatoms, solubilize and mineralize POM and biogenic silica (Smith et al. 1992, Bidle and Azam 1999, Grossart et al. 2004), bacteria appear also important in structuring and decomposing aggregates in tidal flat systems such as the Wadden Sea. These processes, in addition to hydrodynamic forcing, need be included in assessing controlling factors for aggregate dynamics in tidal flat systems. A further indication of intense POC and dissolved polymer hydrolysis is the rather similar concentration of DFAA and DCAA (Table 1, Coffin 1989), supporting the idea that in tidal flat systems high amounts of POC are transformed into DOC (Postma 1981).

Tidal dynamics—Concentrations of most properties assessed varied greatly during tidal cycles, often exceeding the seasonal range of their tidal means. To elucidate systematic tidal patterns, irrespective of the seasonal situation, we normalized the data, showing that SPM, POC, Chl *a*, and aggregate abundance were positively and aggregate ECD negatively correlated to the current velocity with a time lag of 1 h. These notions are in line with previous reports from other tidal flat systems with similar but also other energetic regimes (Chen and Eisma 1995; van Leussen 1996; Fugate and Friedrich 2003). Our normalized tidal cycle, however, in addition shows that individual properties exhibit pronounced differences in their tidal variability, ranging from 70–140% to 30–180% of the tidal mean for Chl *a* and aggregate abundance, respectively (Fig. 3). This normalization provides a valuable tool to compare SPM and aggregate dynamics in tidal systems varying in their energetic properties and SPM characteristics.

Interestingly, and in addition to previous reports, our results indicate that the minima of SPM properties around HT during the day were not as low as during the night and that the aggregate abundance during the day was systematically higher than during the night (Fig. 3). The aggregate ECD did not exhibit such contrasting patterns. This notion points to a light-driven effect on enhanced concentrations of SPM and in particular aggregates during the day. It is well known that in tidal mud flats, benthic diatoms migrate to the surface at LT during the day and photosynthetically produce large amounts of exopolysaccharides (EPS), of which a substantial fraction is water soluble (de Winder et al. 1999; Staats et al. 2000; de Brouwer and Stal 2001). Hence, we assume that parts of the benthic biofilm harboring diatoms and releasing EPS are resuspended at incoming tide during the morning and leading to enhanced concentrations of SPM, POC, aggregates, and Chl *a* as compared to the night, when the benthic diatoms do not migrate to the surface at LT. A support of this assumption is that concentrations of Chl *a* were reduced least during the day and that benthic diatoms are frequently recorded in the water column (Grossart et al. 2004; Stevens et al. 2005). Further, this assumption implies enhanced sedimentation at LT in the evening.

DOC concentrations also exhibited systematic tidal dynamics with minima at HT and maxima at LT, covarying with the number of total bacteria. Dynamics, however, were much less pronounced than those of SPM properties. We assume that the minima at HT were a result of North Sea water, characterized by reduced concentrations of DOC, POC, Chl *a*, and bacterial numbers (M. Lunau and O. Dellwig unpubl. data), coming in through the outlet. The maxima at LT may reflect, at least partly, the injection of pore water from the sediment highly enriched in DOC relative to the water column via tidal pumping.

Seasonal controls of aggregate dynamics—The seasonal variabilities in SPM and aggregate concentrations and characteristics reflected the different energetic conditions but also biological aspects of the growing season. Basically, two

contrasting situations can be distinguished, one reflecting more the fall and winter aspect with low biological productivity and enhanced wind and wave action, and one with high biological productivity. The first one is characterized by high concentrations of SPM and aggregates of a rather small size, low numbers of AGG bacteria per mg SPM, and the second one by elevated Chl *a* concentrations, POC : SPM ratios, but lower concentrations of SPM and aggregates of a larger size. Some aspects of such differences have been reported previously (e.g., Mikkelsen 2002; Fugate and Friedrichs 2003), but the significance of how microbial processes affect aggregation, aggregate dynamics, sedimentation, and the sediment structure in tidal flat systems has been little considered. Our results and observations of the sediment grain-size structure (Chang et al. 2005) indicate that during winter, aggregation is reduced, resulting in a more conservative behavior of suspended aggregates and their size distribution tidally (Fig. 5), higher concentrations of suspended aggregates, lower sedimentation, and strongly reduced particles <63 μm in the surface sediment. In contrast, during the growing season, tidal dynamics of the aggregate size distribution, SPM, POC : SPM, Chl *a*, and bacterial production were much more pronounced (Figs. 4, 5, 6), indicating distinct sedimentation events at slack water. Further, the sediment contained significantly higher amounts of particles <63 μm, implying that they were scavenged in the water column in larger aggregates settling out. We assume that these seasonal differences are mainly due to microbially mediated aggregation and sedimentation during the growing season because of more intense microbial processes and higher production rates of sticky mucus material and EPS during this time (Passow 2002; Bhaskar et al. 2005; de Brouwer and Stal 2001, see previous). Even though water temperature affects its viscosity and thus the sinking rate of aggregates, we assume that this purely physical effect is of little importance and not the only controlling factor for seasonal differences in sedimentation rates of various aggregate fractions, as has been argued recently (Kroegel and Flemming 1998).

We have shown that systematic and recurrent tidal patterns of SPM, aggregate, but also DOC dynamics exist in a tidal flat ecosystem, which is demonstrated best by normalizing the data to their tidal means and relative deviations from it. Applying a new sampling device which serves simultaneously as a settling chamber, we further showed that pronounced differences occur in the quality of various aggregate fractions, affecting their settling properties tidally. Further, our results show that microbial processes are important in affecting aggregate dynamics and sedimentation during the growing season, whereas during fall and winter hydrodynamic forcing is of generally greater importance.

References

BAKKER, D., J. KLIJNSTRA, H. BUSSHER, AND H. VAN DER MEI. 2003. The effect of dissolved organic carbon on bacterial adhesion to conditioning films adsorbed on glass from natural seawater collected during different seasons. Biofouling **19:** 291–297.

BEHRENDS, B., AND G. LIEBEZEIT. 1999. Particulate amino acids in Wadden Sea waters—seasonal and tidal variations. J. Sea. Res. **41:** 141–148.

BHASKAR, P., H. GROSSART, N. BHOSLE, AND M. SIMON. 2005. Production of macroaggregates from dissolved exopolymeric substances (EPS) of bacterial and diatom origin. FEMS Microbiol. Ecol. **53:** 255–264.

BIDLE, K.D., AND F. AZAM. 1999 Accelerated dissolution of diatom silica by marine bacterial assemblages. Nature **397:** 508–512.

CHANG, T., A. BARTHOLOMAE, AND B. FLEMMING. In press. Seasonal dynamics of fine-grained sediments in a back-barrier tidal basin of the German Wadden Sea (southern North Sea). J. Coast. Res.

CHEN, S., AND D. EISMA. 1995. Fractal geometry of in situ flocs in the estuarine and coastal environments. Neth. J. Sea Res. **32:** 173–182.

———, ———, AND J. KALF. 1994. In situ size distribution of suspended matter during the tidal cycle in the Elbe estuary. Neth. J. Sea Res. **32:** 37–48.

CRUMP, B. C., J. A. BAROSS, AND C. A. SIMENSTAD. 1998. Dominance of particle-attached bacteria in the Columbia River estuary, USA. Aquat. Microb. Ecol. **14:** 7–18.

———, AND ———. 2000. Characterisation of the bacterially-active particle fraction in the Columbia River estuary. Mar. Ecol. Prog. Ser. **206:** 13–22.

DE BROUWER, J.F.C., AND L. J. STAL. 2001. Short-term dynamics in microphytobenthos distribution and associated extracellular carbohydrates in surface sediments of an intertidal mudflat. Mar. Ecol. Prog. Ser. **218:** 33–44.

DE WINDER, B., N. STAATS, L. J. STAL, AND D. M. PATERSON. 1999. Carbohydrate secretion by phototrophic communities in tidal sediments. J. Sea Rea. **42:** 131–146.

EISMA, D., AND A. LI. 1993. Changes in suspended-matter floc size during the tidal cycle in the Dollard Estuary. Neth. J. Sea Res. **31:** 107–117.

FERRARI, G. M., F. G. BO, AND M. BABIN. 2003. Geo-chemical and optical characterizations of suspended matter in European coastal waters. Estuar. Coast. Shelf Sci. **57:** 17–24.

FUGATE, D. C., AND C. T. FRIEDRICHS. 2003. Controls on suspended aggregate size in partially mixed estuaries. Estuar. Coast. Shelf Sci. **58:** 389–404.

GROSSART, H., T. BRINKHOFF, T. MARTENS, C. DUERSELEN, G. LIEBEZEIT, AND M. SIMON. 2004. Tidal dynamics of dissolved and particulate matter and bacteria in a tidal flat ecosystem in spring and fall. Limnol. Oceanogr. **49:** 2212–2222.

KIØRBOE, T., AND J. HANSEN. 1993. Phytoplankton aggregate formation: observations of patterns and mechanisms of cell sticking and the significance of exopolymer material. J. Plankton Res. **15:** 993–1018.

KROEGEL, F., AND B. W. FLEMMING. 1998. Evidence for temperature-adjusted sediment distributions in the back-barrier tidal flats of the East Frisian Wadden Sea (southern North Sea), p. 31–41. *In* C. R. Alexander, R. A. Davis, and V. J. Henry [eds.], Tidalites: Processes and products. SEPM Spec. Publ. 61.

LINDROTH, P., AND K. MOPPER. 1979. High-performance liquid chromatographic determination of subpicomol amounts of amino acids by precolumn fluorescence derivatisation with o-phtaldialdehyde. Anal. Chem. **51:** 1667–1674.

LUNAU, M., A. LEMKE, K. WALTHER, W. MARTENS-HABBENA, AND M. SIMON. 2005. An improved method for counting bacteria from sediments and turbid environments by epifluorescence microscopy. Environ. Microb. **7**: 961–968.

———, A. SOMMER, A. LEMKE, H. GROSSART, AND M. SIMON. 2004. A new sampling device for microaggregates in turbid aquatic systems. Limnol. Oceanogr. Meth. **2:** 387–397.

LYNCH, J., J. IRISH, C. SHERWOOD, AND Y. AGRAWAL. 1994. Determining suspended sediment particle size information from

acoustical and optical backscatter measurements. Cont. Shelf Res. **14:** 1139–1165.

MANNINO, A., AND H. R. HARVEY. 2000. Biochemical composition of particles and dissolved organic matter along an estuarine gradient: Sources and implications for DOM reactivity. Limnol. Oceanogr. **45:** 775–788.

MCCANDLISS, R. R., S. E. JONES, M. HEARN, R. LATTER, AND C. F. JAGO. 2002. Dynamics of suspended particles in coastal waters (southern North Sea) during a spring bloom. J. Sea Res. **47:** 285–302.

MIKKELSEN, O. 2002. Examples of spatial and temporal variations of some fine-grained suspended particle characteristics in two Danish coastal water bodies. Oceanol. Acta **25:** 39–49.

———, AND A. PEJRUP 1998. Comparison of flocculated and dispersed suspended sediment in the Dollard estuary, p. 199–209. *In* K. Black, D. Paterson, and A. Cramp. [eds], Sedimentary processes in the intertidal zone. Geol. Soc. London. 139.

MILLIGAN, T. 1995. An examination of the settling behaviour of a flocculated suspension. Neth. J. Sea Res. **33:** 163–171.

MURRELL, M. C., AND J. T. HOLLIBAUGH. 2000. Distribution and composition of dissolved and particulate organic carbon in northern San Francisco Bay during low flow conditions. Estuar. Coast. Shelf Sci. **51:** 75–90.

PASSOW, U. 2002. Production of transparent exopolymer particles (TEP) by phyto- and bacterioplankton. Mar. Ecol. Prog. Ser. **238:** 1–12.

———, AND A. ALLDREDGE. 1995. Aggregation of a diatom bloom in a mesocosm—The role of transparent exopolymer particles (TEP). Deep-Sea Res. II **42:** 99–109.

PLUMMER, D., N. OWENS, AND A. RODNEY. 1987. Bacteria-particle interactions in turbid estuarine environments. Cont. Shelf Res. **7:** 1429–1433.

POSTMA, H. 1981. Exchange of materials between the North Sea and the Wadden Sea. Mar. Geol. **40:** 199–213.

SIMON, M., AND F. AZAM. 1989. Protein content and protein synthesis rates of planktonic marine bacteria. Mar. Ecol. Prog. Ser. **51:** 201–213.

———, H. P. GROSSART, B. SCHWEITZER AND H. PLOUG. 2002. Microbial ecology of organic aggregates in aquatic ecosystems. Aquat. Microb. Ecol. **28:** 175–211.

SMITH, D. C., M. SIMON, A. L. ALLDREDGE, AND F. AZAM. 1992. Intense hydrolytic enzyme activity on marine aggregates and implications for rapid particle dissolution. Nature **359:** 139–142.

STAATS, N., L. J. STAL, B. DE WINDER, AND L. R. MUR. 2000. Oxygenic photosynthesis as driving process in exopolysaccharide production of benthic diatoms. Mar. Ecol. Prog. Ser. **193:** 261–269.

STANEV, E. V., J. O. WOLFF, H. BURCHARD, K. BOLDING, AND G. FLÖSER. 2003. On the circulation in the East Frisian Wadden Sea: Numerical modeling and data analysis. Ocean Dynamics **53:** 27–51.

STEVENS, H., T. BRINKHOFF, AND M. SIMON. 2005. Composition of free-living, aggregate-associated and sediment surface-associated bacterial communities in the German Wadden Sea. Aquat. Microb. Ecol. **38:** 15–30.

TEN BRINKE, W. 1994. Settling velocities of mud aggregates in the Oosterschelde tidal basin (The Netherlands), determined by a submersible video system. Estuar. Coast. Shelf Sci. **39:** 549–564.

TILLMANN, U., K.-J. HESSE, AND F. COLIJN. 2000. Planktonic primary production in the German Wadden Sea. J. Plankton Res. **22:** 1253–1276.

VAN LEUSSEN, W. 1996. Erosion/sedimentation cycles in the Ems estuary. Arch. Hydrobiol. Spec. Issues Advanc. Limnol. **47:** 179–193.

VON TUEMPLING, W., AND G. FRIEDRICH. 1999. Biologische Gewässeruntersuchung. Jena; Stuttgart; Lübeck; Ulm, G. Fischer.

WOLFSTEIN, K., F. COLIJN, AND R. DOERFFER. 2000. Seasonal Dynamics of microphytobenthos biomass and photosynthetic characteristics in the northern German Wadden Sea, obtained by the photosynthetic light dispensation system. Estuar. Coast. Shelf Sci. **51:** 651–662.

Received: 5 May 2005
Accepted: 11 October 2005
Amended: 16 October 2005